地盤と建設
Vol.19, No.1, 2001

Rain-induced groundwater flow experiments in relation to the initiation of shallow landslides in hilly areas

Dissanayake A. Kamalnath (Hiroshima University)
Yasushi SASAKI (Hiroshima University)
Seiji KANO (Hiroshima University)
Desiree Aninon Uy (Hiroshima University)
Takeo MORIWAKI (Hiroshima University)

It is a well-known fact that the topography of hilly or mountainous areas influences the gravity-driven groundwater flow. It has been also observed that the shallow landslides and debris flows due to heavy rains have occurred in the steepest slope encountered just below the summit of mountains or hills even though the actual failure mechanism is not known exactly yet. Small-scale laboratory experiments were carried out using sandy soil on inclined impermeable bed with different inclinations, which closely resembled insitu conditions. Rain-induced groundwater flow was observed to be increasing substantially at the toe of the steepest slope, which eventually led to a toe failure and thereafter a continuing retrogressive failure towards the summit of the slope. The laboratory experiments reported herein elucidate that the convex-concave transition of topography from steep to gentle leads to abrupt change in groundwater flow and thereby causes the toe failure in the steepest slope. Therefore, it is believed that the development of positive pore water pressure and seepage forces in the subsurface could merely explain the mechanism of the occurrence of shallow landslides and debris flows in highly permeable soils.

Keywords: shallow landslide, rainfall, seepage forces, convex-concave change, laboratory experiments, pore pressure (IGC: B3, E4)

1 *Introduction*

It has been reported in many instances around the world that heavy rainfall had caused shallow slope failures in hilly mountainous areas during which the failure materials lose strength and flows (e.g. Brand 1981, Brenner et al. 1985, Ogawa et al. 1987, Costa Nunes et al. 1989, Pradel and Raad 1993, Anderson and Sitar 1995, Dissanayake et al. 1999, Japanese Geotechnical society 1999, Tohari et al. 2000, Sasaki et al. 2001). However, it has been a longstanding ambiguity on the conceptual models of the failure mechanisms of shallow debris flows during precipitation. Some authors, such as Brand 1981,Wolle and Hachich 1989, Fredlund and Rahardjo 1993, Ng et al. 2000, argue that when the failure of a residual soil slope is brought about by rainfall, the mechanism of failure is that water infiltration produces a reduction in matric suction in the unsaturated soils, which leads to the decrease in the effective stress and thereby causing a reduction in shearing strength of soil to a point where equilibrium could no longer be sustained in the slope. Further, they suggest that, as ground water level in most slope failure areas due to rainfall is often well below the ground surface, the positive pore pressures play very little part in the failure mechanism and thus, the failures are more feasible to occur under almost constant total stress and decreasing negative pore pressure. Contrary to the above, many others (for example, Sidle and Swanston 1981, Johnson and Sitar 1990, Wieczorek 1996, Tohari et al. 2000) have well recognized that the rapid infiltration of rainwater and temporary rise in pore water pressures during intense precipitation to be the cause of the failure mechanism of shallow slope failures. However, a few others believe that the debris flows during heavy rainfall mobilize as the principal stress ratio increases due to development of seepage forces; the actual value of principal stress ratio depends on several factors related to seepage including depth of saturation, the seepage orientation and the hydraulic gradient (Iverson and Reid, 1992, Reid and Iverson, 1992, Anderson and Sitar 1995).

Although, many different alternatives have been suggested, the actual mechanism of debris flow initiation is still not known, as most of the researchers who deal with the subject are confined to find solutions to regional problem of debris flow and thereby, have found better solutions, particularly suitable for the area of their concern. The authors have therefore decided to conduct a detailed investigation on shallow landslide initiation mechanism on highly permeable soils. This paper presents the development of model testing apparatus and the results of the tests, as a part of this research.

2 *Landslide at Hiroshima University premises*

The Hiroshima prefecture is mostly underlain by hard rock of granite and hence, hill slopes generally consist of weathered granite soil locally called "Masa" or "Masado" (Igi et al. 1987). The natural forestry on slopes in this region is affected by reforestation activities and at present, mostly pine trees cover the slopes. Hiroshima prefecture, therefore, has many susceptible natural slopes to rain-induced failures and had repeatedly experienced such disasters in many occasions (Sasaki et al. 2001). Out of those, a disastrous event of slope failures occurred recently in June 1999 causing severe damages to property and also human casualties too. This has been lengthily discussed elsewhere (Japan Geotechnical Society 2000) and it had been found that the original slope angle of landslides were in the range of 30~55 degrees. Most of failures were at dented portion of slopes and scarcely at ridge portion. The lengths of 72 % of failed slopes were less than 20m. The failed widths were often less than 15m, and the depths of the failures were mostly less than 2m. Field reconnaissance after the disaster further

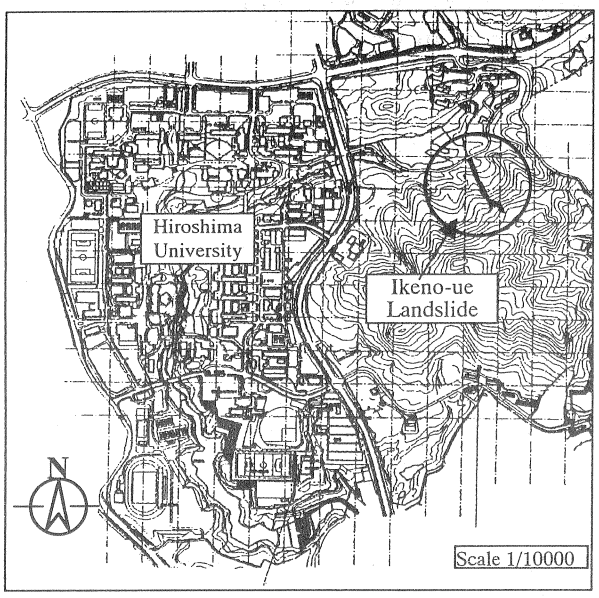

Fig. 1 Location of Ikeno-ue landslide

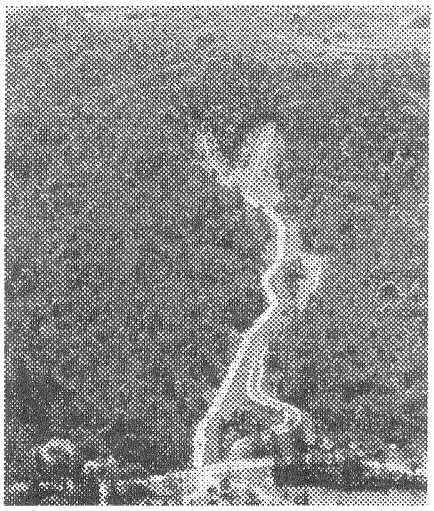

Fig. 2 Aerial photograph of Ikeno-ue landslide after stabilization construction

revealed that the slope failures took place at 1,616 spots in a comparatively small area where the precipitation was intense. Often the sources of the debris flows were shallow slides at the uppermost points of streams. The inclinations and the elevations of most of these failed slopes were in the ranges of 30~45 degrees and 20~600m, respectively. The depth and the area of failed sections were about 1m and 300 m^2, respectively.

The same above-mentioned disaster in June 1999 had caused slope failures in and around the Hiroshima University as well. Serious slope failure took place near Ikeno-ue on the northern slope of Gagara mountain, which spans northwesterly having two visible peaks with elevations of about 320m above mean sea level (MSL). The crest of this landslide rises up to 306m MSL. The total flow length of the slide including source area, main track and depositional area was about 300m and width was varying from about 7.5 to 21m. The depth of the

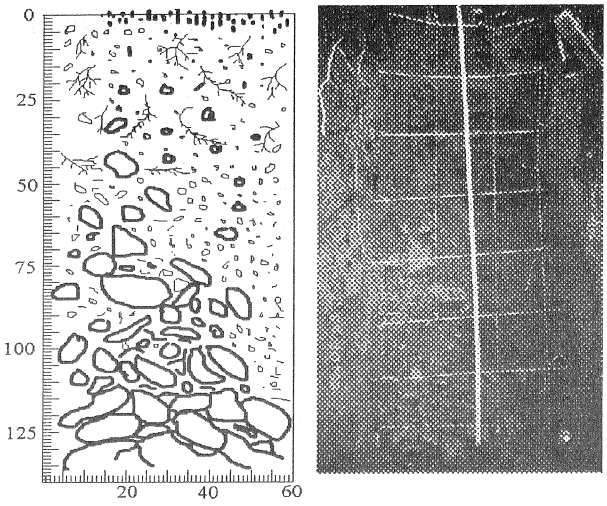

Fig. 3 Sketch of a trial pit at Ikeno-ue slide

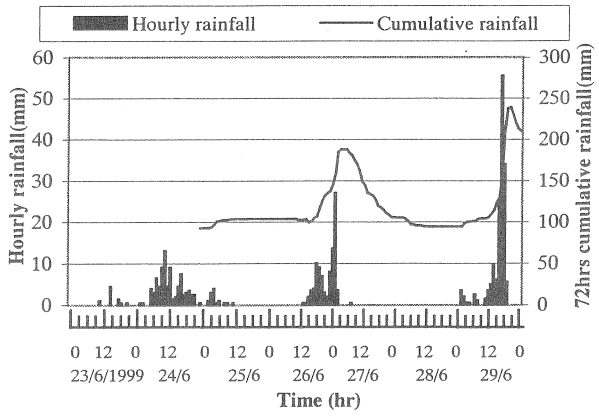

Fig. 4 Rainfall at the site (Hiroshima University station)

failed mass varies from 2.2-3.5m and slide inclination ranges from 25-40 degrees at the source area (Thi Ha 2000). Location and an aerial photograph of the Ikeno-ue shallow landslide site after the remedial construction are shown in Figs. 1 and 2, respectively.

Field investigation of the landslide site showed that the slope consists of extensively weathered Hiroshima Masado. The slope profile basically composed of two layers; the top layer of silty sand with gravel up to a depth of 3.3m and a hard rock of Masado or slightly weathered granite thereafter. The specific gravity of insitu-weathered granite was 2.61. The soil was identified as gravelly sand with uniformity coefficient of 4.5 and D_{10} of 0.42mm. The friction angle and cohesion were found to be 39 degrees and 4kPa, respectively. Sampling pits at the site were subjected for mapping in order to find out the variation of the degree of weathering at depths and one of the results is presented in Fig. 3. The insitu weathering profile of Masado soils at the site was clearly seen from this sketch, which was effectively used in getting an idea of the variation of the rate of percolation of rainwater into the subsoil strata and also in identifying the slides and thereby specifying the possible depth of failure plane.

The variation of rainfall at Hiroshima University is presented in Fig. 4. It shows that the peak rainfall

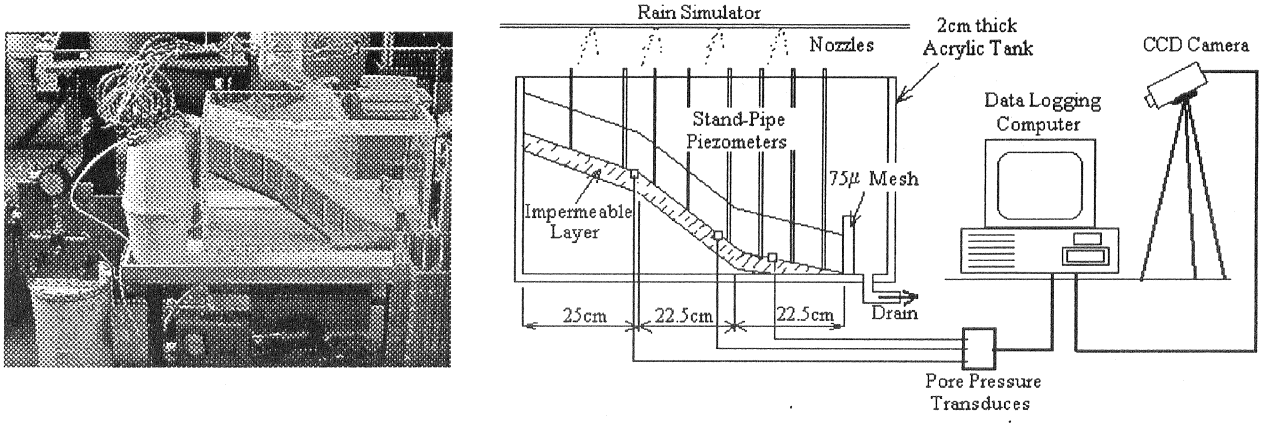

Fig. 5 A view of the apparatus (left) and schematic diagram of the small-scale model test apparatus (right)

occurred from 17:00 to 19:00 on 29th June and thus, the failure was assumed to have initiated within this period. The hourly variation of 72 hours antecedent rainfall is also presented in the same figure and it shows a 72 hours antecedent rainfall of 153.5mm at 17:00. When considering this value with critical rainfall conditions as mentioned by Kaibori & Kuwada (2002), the hourly rainfall must be greater than 50mm/hr for failure to occur. Moreover, the hourly rainfall at 17:00 was 55 mm/hr and therefore, the intensity of rainfall during testing was selected to be 60mm/hr or above.

3 *Development of model test apparatus*

The filed monitoring of moisture movement as a part of the major research, which investigates the failure mechanism of shallow landslide initiation due to rainfall, is carried out at the Ikeno-ue landslide site and thus, the model slope was designed to resemble the scaled dimensions of this site. It is assumed that failure takes place in plain strain condition and therefore, a landslide tank that does not confine the development and occurrence of failure was selected to construct the model slope (Miwa et al. 1997, Enoki 1999, Tohari et al. 2000). As observed from Fig. 3, the hydraulic conductivities of the materials were found to be decreasing as the depth below the ground increased. It was assumed that the bedrock encountered was with low hydraulic conductivity and in the model test the impermeable layer was thus constructed using low permeable children's clay. The steepest slope where failure had taken place at Ikeno-ue landslide was about 44 degrees and therefore, the failure slope was made to be 40 degrees. It is well known fact that not only the precipitation on the landslide area itself matters, but also the rainwater collecting in the catchment area as it feeds the hydro-dynamic flow in the subsurface within the slide area (Sangrey et al. 1984, Ogawa et al. 1987, Karnawati 2000). Therefore, in order to make provisions for such observation, the slope above the failure was also considered in this research and thus, the scaled catchment area above the failed slope was constructed in the landslide tank as shown in Fig. 5.

Johnson and Sitar (1990) had further observed a rapid rise of pore water pressures near the convex-concave transitions of the slope at a debris flow site. Therefore, three pore pressure transducers of each 19.6kPa capacity were buried under the soil at these critical locations. It was found difficult to observe visually the progress of the wetting front and rise of groundwater levels and hence standpipe piezometers were also installed in the model slide tank. Description of the slide tank and the results of the tests carried so far are presented below.

The basic apparatus consists of a landslide tank of 80cm long, 40cm wide and 50cm high. It is made of 2cm thick Acrylic plates and is shown schematically in Fig. 5. The slide model is basically composed of three slopes with 25, 40 and 25 degrees of inclination to the horizontal, respectively, which resembles the topography of Ikeno-ue flow slide (Thi Ha 2000). Acrylic plates with the same inclination support the bottom of the slope and the impermeable bedrock was modeled with children's clay for all the tests. Then as mentioned above, pore pressure transducers and standpipe piezometers were installed as presented in Fig. 5. When placing instruments, the observations of the others (e.g. Johnson & Sitar 1990, Tohari et al. 2000, and Sasaki et al. 2001) were taken into account and these instruments were laid at critical locations to measure changes in groundwater level.

Three pore pressure transducers were buried in the children's clay layer at the bottom boundary of the sand layer before the construction while taking extreme care not to let air bubbles inside them. The tips of all piezometers, which are made of 6mm glass tubes, were protected with 75μm steel meshes in order to block materials flowing into the tubes. The artificial rain was provided through four air-water pressurized nozzles, which had been calibrated to provide desired rainfall intensities. Then, the rainfall simulator was placed above the landslide tank and the predetermined rainfall was applied after preparing the slope with a sandy soil.

The slope throughout the test was video graphed digitally using a CCD (Charged Couple Devices) camera attached to a personal computer as shown in Fig. 5. In addition, markers of different colors were placed on the surface of the sand layer at the toe area of the steepest slope and also on the bottom slope to analyze the movements using digital images taken by the CCD camera.

Data from pore pressure transducers (PPTs) were obtained at one-minute intervals after the start of rain. In

order to maintain the precision, a single value of PPT data was obtained from the average of 101 data points collected within 1 second. Standpipe piezometers were read manually at 2 minutes interval while digital images were taken at a rate of 20 seconds per image throughout the test. Figure 6 shows the location of instruments, the dimensions of installation and the reference numbers of the instruments.

4 *Experimental soil*

Based on tests of Masado soils at Ikeno-ue landslide site, hydraulic conductivity was found to be in the range of 10^{-2}~10^{-3}cm/s. Japan Geotechnical Society (2000) found that the hydraulic conductivities of the sliding materials at different failure sites during June 1999 event ranged between 10^{-2}~10^{-4}cm/s. The direct use of Masado from the site was not possible as the soil contained gravels and the model test was of small scale. Moreover, it had been reported elsewhere (Thi Ha et al. 2002, Tohari et al. 2000) the development of positive pore water pressure before the failure of slopes with high permeable soils. Therefore, in this research it was presumed that the increase of groundwater levels in hillside slopes brings the failure and thus, the soils under consideration would be in the state of saturation. Hence, in this experiment unsaturated soil properties were not taken into consideration. As it could be seen that the hydraulic conductivities were high in these failure areas a sandy soil was selected as the experimental material. Hence, the slope of the sliding mass was constructed using Toyoura sand with following properties. The specific gravity (G_s) of Toyoura sand used in the tests was 2.63. The uniformity coefficient of the sand particle after sieve analysis test was found to be 1.6 with D_{10} of 0.12mm. Maximum and minimum dry densities were 16.7 and 12.7kN/m^3, respectively. Direct shear tests on Toyoura sand samples showed 35 degrees of peak friction angle and cohesion was assumed to be zero as the slope was constructed with disturbed samples of soils. The hydraulic conductivity of Toyoura sand was found to be in the order of 10^{-2}cm/s.

As the pore pressure transducers were in direct contact with the sand layer, it was found to be needed for calibration of those for the optimum moisture content for which they could produce stable readings. Thereby, the most stable readings were found to be given when the initial water content of the samples was 20%. Hence, the sand landslide slope was constructed with the above mentioned initial moisture content. The slopes of 10cm and 5cm thick sand layers were constructed for different tests and extreme care was taken to acquire uniform compaction during construction at each tests. The 10cm thick layer was constructed in 3 layers with each layer giving a uniform compaction with a rammer while 5cm thick sand aquifer by two layers. The model slope was constructed within 30 minutes and samples for initial moisture content tests were taken just before the application of rainfall. However, the calculated void ratios of the slopes for all tests were varying between 0.7~0.9. The volumetric moisture content after the construction of the sand slope was differing in the range of 17~40%, where the most moist slope being the bottom slope.

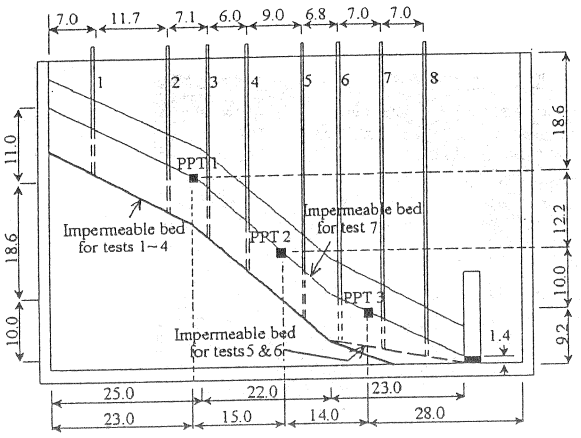

Fig. 6 Locations of the instrumentation in the landslide tank (all dimensions are in cm)

Table 1 Initial condition of the slopes at each test

Test	Slope Position	w %	γ_b kN/m^3	e	θ in %
1	Top	16.3	17.2	0.75	25
	Middle	16.3	17.2	0.75	25
	Bottom	28.6	19.0	0.75	43
2	Top	13.7	16.6	0.78	20
	Middle	17.8	17.3	0.78	26
	Bottom	25.2	18.4	0.78	37
3	Top	15.0	16.5	0.74	23
	Middle	21.1	17.4	0.83	31
	Bottom	26.1	18.2	0.90	36
4	Top	15.1	17.5	0.72	23
	Middle	22.4	18.5	0.72	35
	Bottom	25.7	19.0	0.72	40
5	Top	11.8	15.8	0.84	17
	Middle	19.6	16.9	0.84	28
	Bottom	24.6	17.7	0.84	35
6	Top	12.9	15.9	0.85	18
	Middle	19.8	16.9	0.85	28
	Bottom	26.7	17.9	0.85	38
7	Top	14.4	16.1	0.84	21
	Middle	15.6	16.3	0.84	22
	Bottom	23.4	17.4	0.84	33

5 *Experimental program*

Altogether seven tests were conducted so far and Table 1 represents the details of initial conditions of the constructed slopes before the application of rainfall at each test. After the construction of the slope and just before the application of the rainfall, moisture contents (w) at each slope were tested. Hence, the void ratios (e), bulk densities (γ_b), and initial volumetric water contents (θ) of each slope were calculated using the dimensions of the slopes. The average values of the properties of each slope were then obtained and are shown in Table 1.

Out of the seven tests conducted, Tests 1 to 4 were conducted with the bottom most impermeable layer as shown in Fig. 6 and with a sand-slope thickness of 10cm. Because that the change of the inclination to horizontal at the bottom most part of the model, which then consisted of not three slopes but four, was observed to have an adverse effect on the flow, the bottom slope inclination was changed to 16 degrees as shown by the thick dotted line in Fig. 6 for Tests 5 and 6. It was again found after those tests that the 1.4cm thick mesh frame restricts the flow at the bottom of the slope and virtually leads to a

stagnant water table in this region, which acts similar to a change in slope inclination. Therefore, the slope of the impermeable layer was finally raised to the position shown in Fig. 6, which is similar to the inclinations of the slopes at Ikeno-ue site and on which the Test 7 was conducted. All tests, except Tests 6 and 7, were done with 10 cm thick sand slope. The thickness of the sand slope in Tests 6 and 7 was reduced to 5 cm. Except for the Tests 2 and 3, the intensity of rainfall was set to be 60 mm/hr. Tests 2 and 3 were run at 80 mm/hr rainfall intensity.

6 *Experimental Results*

6.1 *Individual instrument observation*

The pore pressure transducers provided the following changes in pore pressure at the bottom of the sand slopes in each of the tests. From the first look on Figs. 7 to 9, it is very clear that the pore pressures at concave transition region increase very rapidly compared to the top of the slope. Following is the presentation of the PPT and piezometric observations from each test.

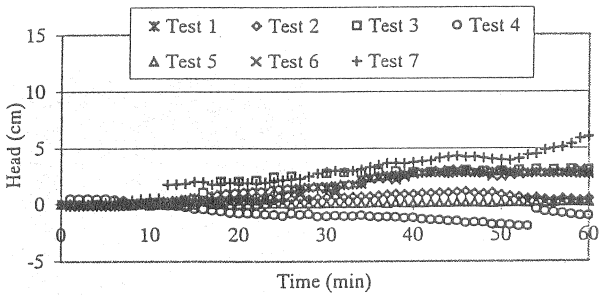

Fig. 7 Pore pressure variation in PPT No. 1 installed at the crest of the middle slope

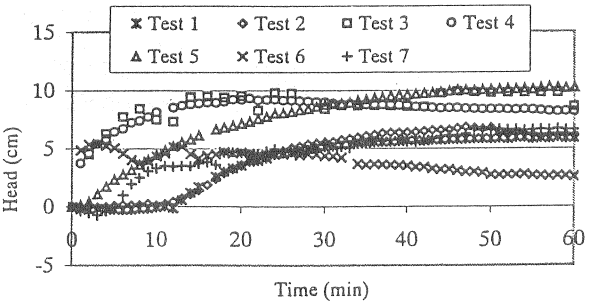

Fig. 8 Pore pressure variation in PPT No. 2 installed at the toe of the middle slope

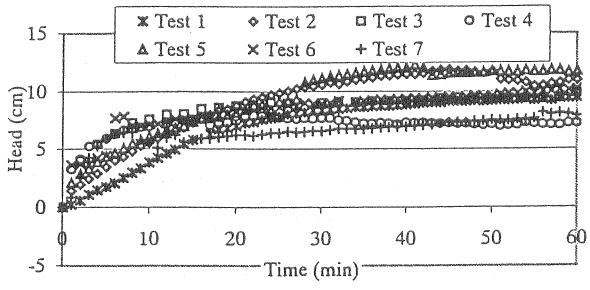

Fig. 9 Pore pressure variation in PPT No. 3 installed just below the inclination changing point in the bottom slope

Though there were 8 piezometers installed in the apparatus, it was unable to recognize any visible variation of the piezometric head in piezometer Nos. 1 to 3. As observed from pore pressure transducer readings, the rest of the piezometers showed groundwater level variation similar to that of PPT's.

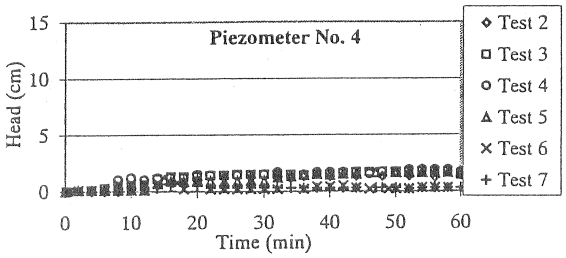

Fig. 10 Piezometric observations of piezometer No. 4

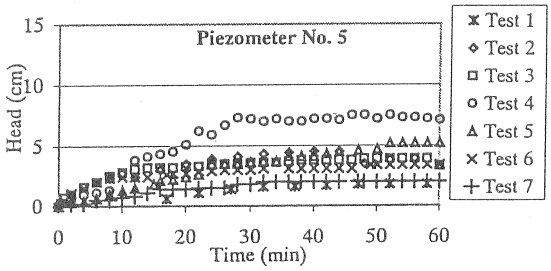

Fig. 11 Variation of piezometric head at piezometer No. 5

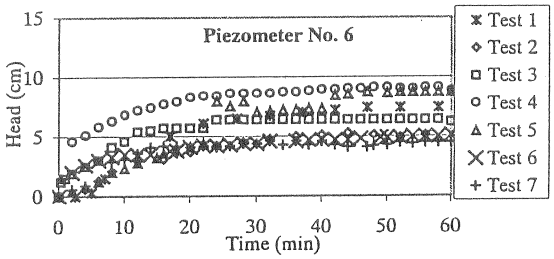

Fig. 12 Variation of piezometric head at piezometer No. 6

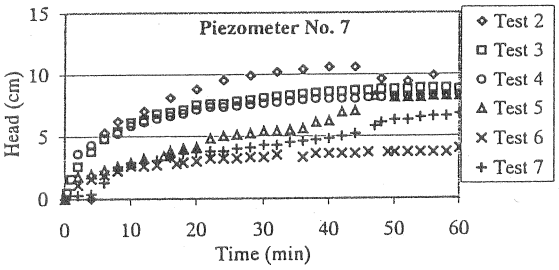

Fig. 13 Piezometric head variation at piezometer No. 7

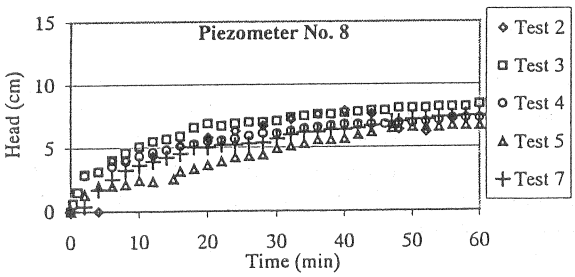

Fig. 14 Piezometric head variation at piezometer No. 8

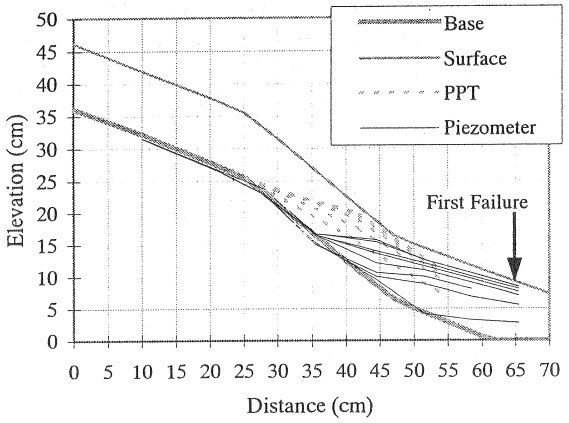

Fig. 15 Groundwater contours at 4 minutes interval during Test 4

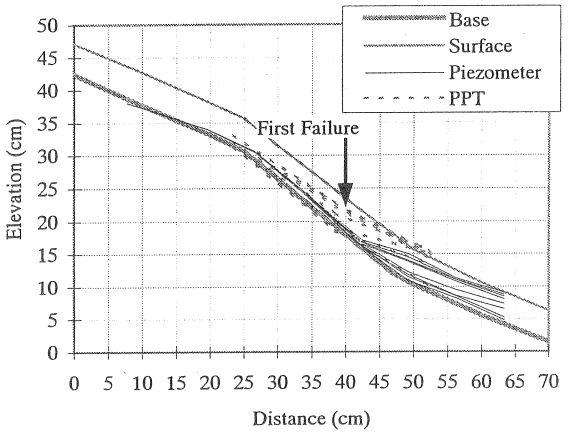

Fig. 16 Groundwater contours at 2 minutes interval during Test 7

In order to see the groundwater level variation with time after the application of rainfall, above observed piezometric and pore pressure transducer readings were plotted along the slope as shown in the Figs. 15 and 16. In Fig. 15, both the piezometric and PPT head contours were drawn for 4 minutes interval starting from the application of rain at time, t=0. A gradual increment of head towards the surface of the sand layer could be observed. The first failure of this test was observed after 23 minutes of rain and the contours are therefore shown until 24 minutes in Fig. 15. Similarly, the contours were drawn for all seven tests and Fig. 16 represents those for Test 7. Here, the first failure occurred after 14 minutes rainfall and thus, the contours of 2 minutes interval up to 14 minutes are shown.

Besides the individual observations of piezometers and pore pressure transducers, it is much more clear from the above Figs. 15 and 16 that the groundwater level abruptly increases in the region closer to the convex-concave slope transition region.

6.2 *Development of failure*

It was manually surveyed the failure development while the CCD camera was recording digital images of the slope throughout the test. The first failure details including the time of occurrence, the location, the progress and the descriptions are given in Table 2. The distance for the failure was measured from the bottom of the left corner of the landslide tank as shown in Fig. 6.

Table 2 Description of failure in each test

Test	Time for First failure (min)	Distance for first failure (cm)	Remarks
1	104	49	Leaking of water and sand under the filter, Retrogressive failure
2	47	63	Leaking of water and sand under the filter, collapse of soil
3	13	60	Slide, Retrogressive failure
4	23	65	Slide, Retrogressive failure
5	64	55	Subsidence, Retrogressive failure
6	10	50	Slide, Retrogressive failure
7	14	40	Slide, Retrogressive failure

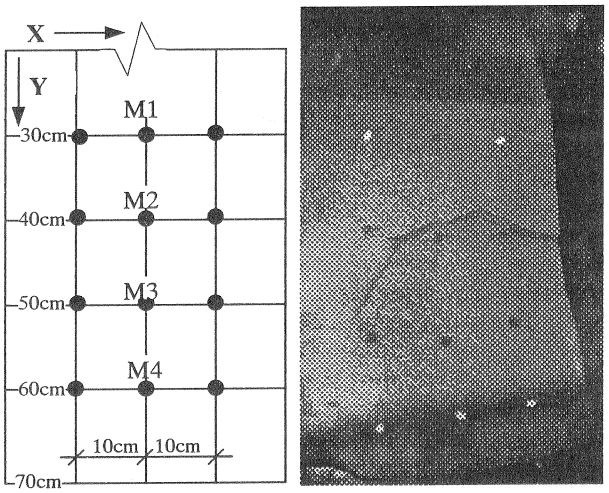

Fig. 17 Array of markers and failure in Test 7

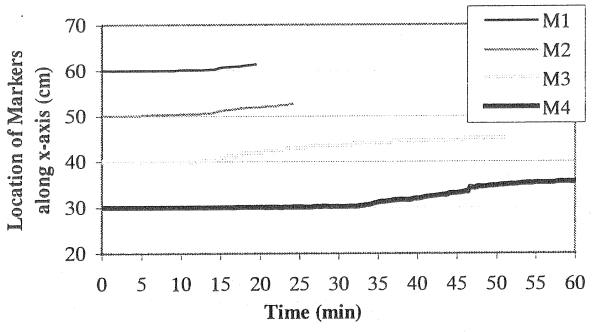

Fig. 18 Locations and displacements of markers M1~M4 along Y-axis

It has been observed during Tests 1 to 6 that the failure initiated above the middle portion of the bottom slope near the toe of the steeper slope. Tests 1 and 2 were done with a filter-frame just placing at the edge of the tank, which led to wash the sand away underneath the frame. Later, the frame was glued to the tank and much better results were obtained. All the failures were sliding type, which retrograded towards the summit of the steeper slope. A typical first failure observed during Test 7 is presented in Fig. 17.

The positions of the markers and a still image of their movement during Test 7 are given in Fig. 17. These markers were placed on the surface of the slope over the possible region of failure with the experience from previous tests.

The results of the change of locations of markers obtained from digital images taken by CCD camera are presented in Fig. 18 together with their initial positions at the start of the rainfall when t=0. This figure shows the movement analysis of markers M1 to M4 along the Y-axis down the slope (see Fig. 17) from the digital images taken continuously throughout the Test 7. The movement along the X-axis, across the slope, was found negligible.

7 *Discussion of the results*

The slope was basically instrumented to measure the variation of groundwater level using pore pressure transducers and standpipe piezometers. The failure of the slope during testing was digitally photographed using a CCD camera and the results obtained for seven tests were presented above. The causes for these observations could be analyzed and interpreted as follows.

7.1 *Groundwater flow*

The initially high moisture content used in the slope construction of the sand layer has been seen redistributed amongst slopes leaving bottom slope with higher saturation (Table 1). On the contrary, the top slope was seen to be the driest compared to the middle slope. The void ratios of constructed slopes for above tests showed that Test 4 has the most densely packed soils while Test 6 was having the largest void ratio. Therefore, higher suction can be expected in the sand slope in Test 4 and as a result, the pore water pressure transducer reading at the top slope showed continuous negative pressure throughout the test (Fig. 7).

Moreover, piezometer Nos. 1 and 2 showed no increment at all during all tests despite the variation of the thickness of the sand layer. However, it has been observed (Figs. 8 and 10) that when the sand layer is thicker then there is a greater time lag between the start of the rain and the wetting front to reach the impermeable layer. When the soil was nearly saturated then it has been seen that the increment of pore water pressure (Fig. 9) and piezometric head (Figs. 11 to 15) was almost instantaneous.

The non-saturation of the top slope is considered to be attributed to two major factors. Firstly, the quick saturation of the top layers of the sand creates unsaturated flow above the impermeable layer, which eventually touches the bottom of the slope at the steeper slope and thereby, the recharge of rainfall accumulates along the down slope for movement (Miyazaki 1993). Second is found to be the entrapment of air flowing upwards towards the summit of the slope and thereby causing a barrier to enter water to the depths of the soil. The above are only the possibilities of what could have happened in the upper slope and hence, more detailed investigation is needed to explain this observed behavior.

It has been also observed that there was a general tendency for pore pressure transducers to read higher values than piezometric reading in almost all the tests (Figs. 15 and 16). Even though it has not been established a solid reason for this observation yet, it is suspected that the increase of weight of the soil during precipitation and the time lag in response of flow type instruments like piezometers for the measurements of increment of groundwater level could lead to the difference of piezometric and pore pressure transducer reading at a particular time of measurements.

Taking into consideration the above observation, an analysis of unconfined groundwater flow over an inclined impermeable bed was done assuming homogenous soil properties of the sand aquifer and Dupuit-Forchcheimer considerations on the direction of flow. In addition during the saturated flow, precipitation was assumed to be percolated instantaneously and readily available for flow along the thickness of the flow domain. The governing partial differential equation was then found to be (referring to Fig. 19)

$$(h-b)\cos^2\beta\frac{\partial^2 h}{\partial x^2}+\left(\frac{\partial h}{\partial x}\right)^2\cos^2\beta-\frac{\partial b}{\partial x}\cdot\frac{\partial h}{\partial x}\cos^2\beta+\frac{N}{K}=\frac{n_e}{K}\frac{\partial h}{\partial t} \quad (1)$$

where h is the height of the water table above a datum, b is the height of the impermeable bed, β is the inclination of the impermeable bed to the horizontal, N is the precipitation, K is the hydraulic conductivity of aquifer medium, n_e is the effective porosity of the medium and t is the time elapsed (Fig. 19)

The above highly non-linear partial differential equation was solved using explicit finite difference formulation, which was programmed using FORTRAN language, and also problem-specific boundary and initial conditions. The results of the application of above solution procedure to the Test 7 are presented in Fig. 20.

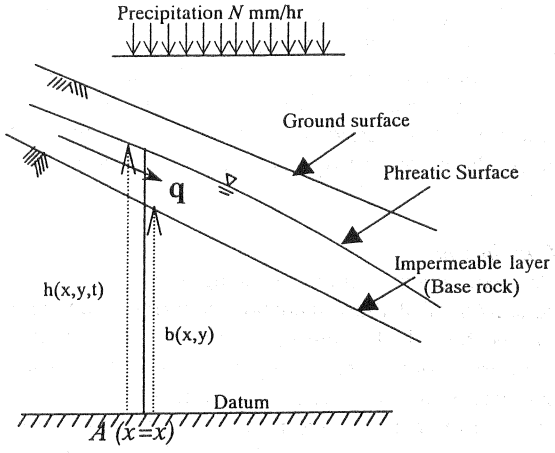

Fig. 19 A schematic view of an inclined phreatic aquifer

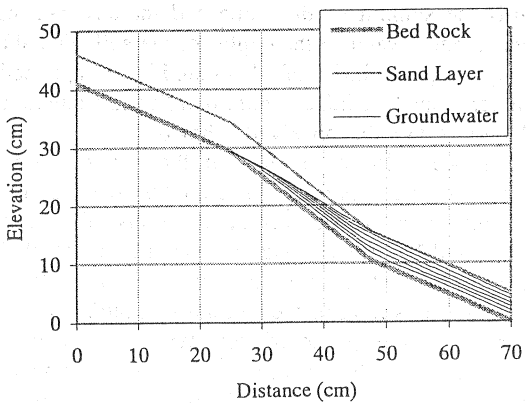

Fig. 20 Analytical results of groundwater flow variation for 60mm/hr rainfall (Hydraulic conductivity was 0.02cm/s, effective porosity was 0.43). Contours are drawn in 2-minute interval starting from the 4th minute.

It could be seen from Fig. 20 that the water level was steadily increasing in the bottom slope having higher rate of increase near the convex-concave transition region. The increase of water level in piezometers at the bottom slope during Test 7 (Fig. 16) was similar to the analytical results and was found to be due to higher state of saturation before the beginning of the artificial recharge by rainfall. However, the initial non-saturation of soil in the steeper slope had caused a deviation of the observed groundwater flow from the analytical results.

7.2 *Failure mode of the slope*

The collapse of slopes in almost all the tests was a sliding failure that was retrograded towards the summit of the slope. The first failure had been observed in all tests, except the Tests 1 and 7, just in the vicinity of the most adverse convex-concave slope transition region. In Tests 2 to 4, the most abrupt slope transition region was where the 25-degree slope changed to horizontal at 60 cm distance (Fig. 15). Similarly in Test 7 the only convex-concave change in slope was at 47.5 cm distance and thus, the water pressure in this region was found to be increasing in this region and toe failure was the result. Figure 17 shows the first failure of the slope during Test 7 while the movements of surface markers with time is given in Fig. 18. These figures clearly show that the marker nos. M2, M3 and M4 have started to move at once on 14th minute after the start of the test due to the pore pressure and seepage forces at the toe of the slope. Marker M1 has started to move on 32nd minute, which clearly shows the retrogressive nature of failure of the slope.

8 *Conclusions*

An experimental study is being done to clarify the mechanism of shallow landslide occurrence on inclined impermeable beds during rainfall. A small-scale laboratory model testing apparatus was built and the slope was basically instrumented to measure the variation of groundwater level using pore pressure transducers and standpipe piezometers. The failure of the slope during testing was digitally photographed using CCD camera and the results obtained after 7 tests and their implications on the instability of the highly permeable soils were presented in this paper.

It was first found that irrespective of the thickness of the sand slope, most of the top slope remained in the unsaturated state during testing. This was considered to be attributed to two major factors as mentioned under the section 6.1. First is due to the occurrence of unsaturated flow above the impermeable layer. The second is found to be caused by the entrapment of air flowing upwards towards the summit of the slope. However, it is felt that a detailed investigation is needed to explain this observed behavior.

Pore pressure transducers were found to be showing higher values of pore pressure than the hydrostatic pressure, which was supposed to be measured (see section 6.1). Therefore, when using pore pressure transducers in measuring the ground water level in flowing condition, extreme care must be taken in interpreting them. Though there is a time lag in piezometric observation, it is found to be the most feasible method to measure the height of free surfaces within a highly permeable material, especially for small-scale laboratory model testing apparatus.

Mainly, it was found both experimentally and from numerical analysis that the groundwater flow near the convex-concave slope transition region increased abruptly and lead to the first failure, which eventually retrograded by multiple slides towards the crest.

References

1. Anderson, A. and Sitar, N., Analysis of rain-induced debris flows, Journal of geotechnical engineering, ASCE, Vol. 121, No. 7, pp. 544-552, 1995.
2. Brand, E. W., Some thoughts on rain-induced slope failures, Proceedings of the 10th International Conference of Soil Mechanics and Foundation Engineering, Stockholm, Vol. 3, pp. 373-376, 1981.
3. Brenner, R. P., Tam, H. K. and Brand, E. W., Field stress path simulation of rain-induced slope failure, Proceedings of the 11th International Conference of Soil Mechanics and Foundation Engineering, San Francisco, Vol. 2, pp. 991-996, 1985.
4. Costa Nunes, A. J., Couto Fonseka, A. M., Fernandus, C. E. de M. and Craizer, W., Intense rainstorms and ground slides, Proceedings of the 12th International Conference of Soil Mechanics and Foundation Engineering, Rio de Janeiro, pp. 1627-1630, 1989.
5. Dissanayake, A. K., Sasaki, Y. and Seneviratne H. N. Threshold rainfall for Bereagala landslide in Sri Lanka, Proceedings of the International Symposium on Slope stability Engineering, Matsuyama, pp. 495-500, 1999.
6. Enoki, M., Slope surface failure caused by precipitation, Soils and Foundation Vol. 47, No. 5, pp. 17-20, 1999.
7. Fredlund, D. G. and Rahardjo, H., Soil mechanics for unsaturated soils, John Willy and Sons, Inc., New York, pp.340-345, 1993.
8. Igi, S., Murakami, N. and Okubo, M. (editors), Regional Geology of Japan, Part 7, Chugoku, Kyoritsu Shuppan Co. Ltd., p. 290, 1987, (in Japanese).

9. Iverson, R. M. and Reid, M. E., Gravity-driven groundwater flow and slope failure potential, 1. Elastic effective stress model, Water Resources Research, Vol. 28, No. 3, pp. 925-938, 1992.
10. Japanese Geotechnical Society, Special report on the disaster due to heavy rainfall in Hiroshima prefecture p. 222, 2000 (In Japanese).
11. Johnson, K. A. and Sitar, N., Hydrologic conditions leading to debris flow initiation, Canadian Geotechnical Journal, Vol. 27, pp. 789-801, 1990.
12. Kaibori, M. and Kuwada, S., Some features of debris flow movements from the view point of disaster prevention, Proceedings of the 14th Southeast Asian Geotechnical Conference, Hong Kong, 2002 (in print)
13. Karnawati, D., Assessment on mechanism of rain-induced landslides by slope hydrodynamic simulation, Proceedings of GeoEng2000 Melbourne, Australia, 2000, (CD Rom version).
14. Miwa K., Cho, K. and Hira, M., Stability of Shirasu talus deposits due to inflow and outflow normal to slope, Soils and Foundation, Vol. 37, No. 4, pp. 127-131, 1997.
15. Miyazaki, T., Water flow in soils, Marcel Dekker Inc., p. 296, 1993.
16. Ng, C. W. W., Tung, Y. K. and Liu, J. K., 3D analysis of rainfall paterns on pore water pressures in unsaturated slopes, Proceedings of GeoEng2000 Melbourne, Australia, 2000, (CD Rom version).
17. Ogawa, S.,Ikeda, T., Kamei, T. and Wada, T., Field investigation of seasonal variations of ground water levels and pore water pressure in landslide areas, Soils and Foundations, Vol. 27, No. 1, pp. 50-60, 1987.
18. Pradel, D. and Raad, G., Effect of permeability on surficial stability of homogeneous slopes, Journal of geotechnical engineering, ASCE, Vol. 119, No. 2, pp. 315-332, 1993.
19. Reid M. E. and Iverson, R. M., Gravity-driven groundwater flow and slope failure potential, 2. Effects of slope morphology, material properties and hydraulic heterogeneity, Water Resources Research, Vol. 28, No. 3, pp. 939-950, 1992.
20. Sangrey, D. W., Harrop-Williams, K. O. and Klaiber, J., Predicting ground water response to precipitation, Journal of geotechnical engineering, ASCE, Vol. 110, No. 7, pp. 957-975, 1984.
21. Sasaki, Y., Moriwaki, T. & Kano, S., Rainfall index for warning against slope failure disaster, Proceedings of the 15th International Conference on Soil Mechanics and Geotechnical Engineering, Istanbul, pp. 1249-1252, 2001.
22. Sidle, R. C. and Swanston, D. N., Analysis of small debris slide in coastal Alaska, Canadian Geotechnical Journal, Vol. 19, pp.167-174, 1981.
23. Thi Ha, Study of effect of rainfall to the stability of Masado slopes, Graduation thesis, Faculty of Engineering, Hiroshima University, Japan, p. 70, 2000, (in Japanese)
24. Thi Ha, Moriwaki, T., Sasaki, Y., Kano, S. and Dissanayake, A. K., Field measurements of moisture content and suction in Masa slope at Hiroshima university campus, Journal of Ground Engineering (Jiban to Kensetsu), Japanese Geotechnical Society, Chugoku Branch, 2001, (in print, in Japanese).
25. Tohari, A., Nishgaki, M. and Komatsu, M., Laboratory experiments on initiation of rainfall-induced slope failure with moisture content measurements, Proceedings of GeoEng2000 Melbourne, Australia, 2000, (CD Rom version).
26. Wieczorek, G. F., Landslide triggering mechanisms, Landslide investigation and mitigation, Special report 247 (Turner, A. K. and Schuster, R. L., eds.), National Academy Press, Washington D. C., pp. 76-90, 1996.
27. Wolle, C. M. and Hachich, W., Rain-induced landslides in southern Brazil, Proceedings of the 12th International Conference of Soil Mechanics and Foundation Engineering, Rio de Janeiro, pp.1639-1642, 1989.